Vibrational properties of the mixed mass modulated spring chain: thermodynamic properties and Doppler shift

1990 J. Phys.: Condens. Matter 2 7407

(http://iopscience.iop.org/0953-8984/2/36/004)

J. Phys.: Condens. Matter 2 (1990) 7407–7423. Printed in the UK

Vibrational properties of the mixed mass modulated spring chain: thermodynamic properties and Doppler shift

Stephen W Lovesey† and David R Westhead‡

† Rutherford Appleton Laboratory, Chilton, Didcot, Oxon, OX11 0QX, UK and Institute of Physics, University of Uppsala, Uppsala, Sweden

‡ Department of Theoretical Physics, University of Oxford, Oxford OX1 3NP, UK

Received 1 March 1990

Abstract. Thermodynamic properties of the modulated spring chain, introduced by de Lange and Janssen to study excitations in an incommensurate composite system, are obtained by an exact algebraic method. A new feature is the inclusion of a mass defect. It is shown that a light mass defect enhances effects due to spring modulation, which are most significant at low temperatures.

1. Introduction

We report an extensive study of the vibrational properties of a chain of atoms bound by harmonic forces in which the springs depend on site position. In the most general case considered, the mass of one atom is taken to be different from all others. Our analysis of the mixed mass chain is exact at all stages.

The motivation for the study is twofold. First, it is a study in statistical mechanics of an exactly solvable model that can be viewed as a nontrivial generalisation of the Rubin (1961) model, in which the springs are independent of the site position. Secondly, the results might serve as a feasibility study for experiments designed to unravel the lattice dynamics of incommensurate crystals. In this context, the model with equal masses was introduced by de Lange and Janssen (1981) and it is usually referred to as the modulated spring model (Currat and Janssen 1988). Our contribution to its study is an exact analytic formulation of the vibrational properties, which complements and extends previous results largely obtained by numerical techniques; for a review see Currat and Janssen (1988). Armed with an analytic formulation it is possible to study exactly properties induced by a single defect. We choose a simple mass (isotope) change, as in the Rubin model. A preliminary account of our work has been published (Lovesey 1989), and a companion to this paper reports the dual spectrum and inelastic neutron cross section (Lovesey and Westhead 1990).

The site dependence of the springs mimics the situation prevailing in an incommensurate composite system. In this instance, spacing of the atoms in the chain is not the same as that between atoms in the crystal in which the chain is embedded. Hence, the local environment of atoms in the chain varies from site to site, and it is taken to produce springs that depend on site position. This dependence is assumed to embody the entire influence on the chain of the crystal which it inhabits.

0953-8984/90/367407+17$03.50

The potential energy in the model is

$$\frac{1}{2}\sum_n \alpha_n (u_n - u_{n-1})^2. \tag{1}$$

Here, u_n is the displacement of the atom at the site labelled by the integer n, and α_n is the spring constant. Following de Lange and Janssen (1981) we adopt the form

$$\alpha_n = m\{\alpha - \gamma \cos(nQ + \Delta)\} \tag{2}$$

in which the strength γ, phase Δ and wavevector Q specify the sinusoidal modulation. The spacing between atoms in the chain is equal to unity, and m is the atomic mass. In the companion paper (Lovesey and Westhead 1990) the properties of both cosine and squared-cosine modulations are discussed in the context of the one-phonon neutron cross section.

In our work $Q = (2\pi M/N)$ where M and N are integers, i.e. the springs are N-fold periodic $\alpha_{n+N} = \alpha_n$. By a suitable choice of M, N we can obtain the modulation wavevector appropriate to an interpretation of numerical or experimental data, since the value of Q is specified with finite accuracy. An incommensurate system can be approached by employing a sequence of fractions, e.g. Fibonacci numbers, but we do not pursue this topic. Given that the equation of motion for the displacements is one-dimensional and the springs are periodic, the lattice dynamics in the form of a displacement Green function can be derived analytically. The model is specified fully in section 2, and calculation of the displacement Green function is taken up in section 3.

Local properties of the chain are revealed in the second-order Doppler shift of a Mössbauer peak. In order to explore what information might emerge from appropriate experiments, we introduce a single mass defect in the model to represent a Mössbauer isotope. It is well known that the displacement Green function of the mixed mass system can be expressed in terms of the Green function of the pure system, and appropriate expressions are provided in section 4. High- and low-temperature series for the mean square velocity of the mass defect and the defect energy are reported in section 5. Impurity induced effects in the density of states are summarised in section 6. Extensive numerical results are discussed in section 7. Our conclusions are summarised in section 8.

2. Equation of motion and correlation functions

The Hamiltonian which describes the modulated spring model is the sum of kinetic and potential energy (1) terms. This Hamiltonian is diagonalised by normal modes labelled by the index σ, with eigenvectors and eigenfrequencies denoted by $f_\sigma(n)$, ω_σ respectively. The orthonormality and closure relations are taken to be

$$\sum_n f_\sigma(n) f_{\sigma'}(n) m_n = \delta_{\sigma,\sigma'} \tag{3}$$

and

$$\sum_\sigma f_\sigma(n) f_\sigma(n') = \delta_{n,n'}/m_n \tag{4}$$

where m_n is the mass of the atom at site n. If b_σ, b_σ^+ are standard Bose operators then the displacement operator is

$$u_n = \sum_\sigma f_\sigma(n)(b_\sigma^+ + b_\sigma)/\sqrt{2\omega_\sigma}. \tag{5}$$

It is convenient to couch the lattice dynamics in terms of the displacement Green function

$$P(l,n;z) = \sum_\sigma f_\sigma(l) f_\sigma(n)/\{z^2 - \omega_\sigma^2\} \tag{6}$$

where $\mathrm{Re}\, z = \omega$ and $\mathrm{Im}\, z = \eta > 0$. The equation of motion for $P(l,n;z)$ is readily shown to be

$$(mz^2 - \alpha_l - \alpha_{l+1})P(l,n;z) = \delta_{l,n} - \alpha_l P(l-1,n;z) - \alpha_{l+1} P(l+1,n;z). \tag{7}$$

The calculation of $P(l,n;z)$ with N-fold periodic springs (2) is the subject of the next section.

We conclude this section by recording expressions, written in terms of the Green function, for correlation functions of immediate interest. First, the time-dependent displacement correlation function

$$\langle u_n u_l(t)\rangle = -\frac{1}{\pi}\int_{-\infty}^{\infty} \mathrm{d}\omega\{1 + n(\omega)\}\exp(\mathrm{i}\omega t)\,\mathrm{Im}\, P(l,n;\omega). \tag{8}$$

Here, the imaginary part of the Green function is calculated in the limit $\eta \to 0$, $n(\omega)$ is the Bose factor at temperature T ($\hbar = k_B = 1$)

$$n(\omega) = \frac{1}{\exp(\omega/T) - 1} \tag{9}$$

and the angular brackets denote a thermal average of the enclosed quantity.

The velocity correlation function, required for the proposed Mössbauer experiment and total energy calculation, can be calculated from (8). However, the N-fold periodicity of the springs fragments $\mathrm{Im}\, P$ in to N pieces and this structure renders evaluation of the integral a complicated task. In view of this, we exploit the identity

$$2n(\omega) + 1 = 2\omega T \sum_{k=-\infty}^{\infty} \frac{1}{\omega^2 + r_k} \tag{10}$$

where k is an integer and $r_k = (2\pi k T)^2$ to obtain the result

$$\langle v_l v_n\rangle = T \sum_{k=-\infty}^{\infty} \{(\delta_{l,n}/m) + r_k P(l,n;z^2 = -r_k)\}. \tag{11}$$

Expressions (8) and (11) are presented for the equal-mass chain. They are valid for the mixed-mass system, discussed in section 4, when P is replaced by the appropriate Green function and the mass m in (11) is replaced by m_l, the mass at the site labelled by l.

3. Green function

In this section we obtain an analytic expression for the Green function (6) using the equation of motion (7). The mathematical method employed is described in previous publications (Lovesey 1988a, b) so only an outline of the calculation is presented here, with some details deferred to an appendix. The reader should note that the derivation is independent of the specific form of the spring modulation given in (2); it is only required to be N-fold periodic.

We aim to calculate the site-diagonal Green function $P(n;z) \equiv P(n,n;z)$. From (7) it is readily shown that this quantity can be written in terms of two infinite continued fractions. For N-fold periodic springs the two continued fractions are proportional to each other, and expressible in terms of two sets of polynomial functions denoted here by $\{p_n\}$ and $\{q_n\}$. These functions are constructed recursively from the difference equation

$$p_{n+1}(z^2 - \alpha_n - \alpha_{n+1}) + p_n\alpha_n^2 + p_{n+2} = 0 \tag{12}$$

with a similar equation for q_n, and initial conditions $p_0 = q_1 = 0, p_1 = q_0 = 1$. The Wronskian relation is

$$p_{n+1}q_n - p_nq_{n+1} = \begin{cases} 1 & n = 0 \\ \alpha_{n-1}^2\alpha_{n-2}^2 \ldots \alpha_0^2 & n \geq 1. \end{cases} \tag{13}$$

Let us define

$$D_N = (2\alpha_{N-1}\alpha_{N-2}\ldots\alpha_0)^2 - (p_{N+1} + q_N)^2 \tag{14}$$

then the result for the site-diagonal Green function can be written

$$mP(n;z) = \frac{\pm(q_{N+1}p_{n+1}^2 + p_{n+1}q_{n+1}(q_N - p_{N+1}) - p_Nq_{n+1}^2)}{\alpha_n^2\alpha_{n-1}^2\ldots\alpha_0^2\sqrt{-D_N}}. \tag{15}$$

Hence, the displacement Green function for an N-fold modulation is fully determined by a knowledge of the functions $\{p_n\}$, $\{q_n\}$ up to p_{N+1}, q_{N+1}. The choice of sign in (15) is discussed in an appendix.

A formula for the density of states $Z(\omega)$, normalised to unity in the interval $0 \leq \omega < \infty$, is obtained from the definition of the Green function (6). We find,

$$Z(\omega) = -\frac{2\omega}{\pi N}\sum_{n=0}^{N-1} m \ \mathrm{Im}\, P(n;\omega) \tag{16}$$

and the result is valid for the mixed mass system when the appropriate Green function is substituted and the mass is replaced by m_n. Substituting (15) in (16) the sum over sites can be accomplished with the Christoffel–Darboux formula. The final expression for the density of states of the equal-mass, N-fold periodic spring chain is

$$Z(\omega) = \begin{cases} 0 & D_N < 0 \\ \dfrac{2\omega|p'_{N+1} + q'_N|}{\pi N\sqrt{D_N}} & D_N \geq 0 \end{cases} \tag{17}$$

where the prime denotes differentiation with respect to $z^2 = \omega^2$. General features of the analytic structure of (17) have been discussed in detail (Lovesey 1988a, b), together with an explicit expression for $N = 3$ (Lovesey 1989). Further examples are presented and discussed in section 6, including the effect of a simple mass defect which is introduced in the following section.

4. Mass defect

It is well established that a mass defect has a significant effect on the lattice dynamics of a harmonic system; see, for example, Maradudin *et al* (1971). Here we examine an essentially new model in which a mass defect is substituted in a chain with modulated springs, specified by (2). This model is of interest in statistical physics as a generalisation of Rubin's model. However we are interested in it chiefly as a model to elucidate features of an incommensurate crystal which might be revealed in the second-order Doppler shift of a Mössbauer peak. If the isotope is placed at the site labelled s the shift is proportional to the mean-square velocity $\langle v_s^2 \rangle$. This quantity is calculated from (11) with the appropriate Green function.

The latter is derived from an equation of motion obtained from (7) by replacing the mass on the left-hand side by $m(1-\lambda\delta_{l,s})$; here the mass defect parameter $\lambda = 1-m'/m$ where m' is the mass of the isotope. Note that for a light defect $0 \leq \lambda \leq 1$, while for a heavy defect $\lambda < 0$. The displacement Green function $G(l, n; z)$ can be expressed in terms of the Green function $P(l, n; z)$ for the equal-mass chain. A standard calculation leads to the result (see, for example, Lovesey 1986)

$$G(l,n;z) = P(l,n;z) + \frac{m\lambda z^2 P(l,s;z)P(s,n;z)}{1 - m\lambda z^2 P(s;z)}. \tag{18}$$

The density of states calculated from (18) for site-independent springs ($\gamma = 0$ in (2)) shows that a heavy mass decreases normal mode frequencies from their values in the corresponding pure ($m = m'$) case, whereas a light defect increases frequencies and generates localised modes outside the band interval of the pure density of states. Results for modulated springs are presented in section 7.

The mean-square velocity of the isotope is calculated using (11) with $m \rightarrow m_l$ and (18), taking $l = n = s$ and $m_s = m'$. We find,

$$m'\langle v_s^2 \rangle = T\left[1 + \frac{2}{\lambda}\sum_{k=1}^{\infty}\left\{1 + \frac{\lambda - 1}{1 + m\lambda r_k P(s; z^2 = -r_k)}\right\}\right] \tag{19}$$

where $r_k = (2\pi kT)^2$, and the pure Green function is given by (15). This expression is the basis of high- and low-temperature expansions presented in the next section, and numerical work reported in section 7.

For a harmonic system, the total internal energy is $\sum_l m_l \langle v_l^2 \rangle$. We are particularly interested in the contribution from the defect. An appropriate expression for the defect energy per particle $\varepsilon(s)$ is obtained from (11) with $m \rightarrow m_l$ and (18) together with the standard identity,

$$m\sum_n P(s,n;z)P(n,s;z) = -P'(s;z) \tag{20}$$

where $P(s;z) \equiv P(s,s;z)$, the sum is over all sites the and the prime denotes differentiation with respect to z^2. After some straightforward algebra we find the result

$$\varepsilon(s) = -\frac{2T}{N_0}\sum_{k=1}^{\infty} z^2 \frac{\mathrm{d}}{\mathrm{d}z^2}\ln[1 - m\lambda z^2 P(s;z)] \tag{21}$$

in which the function is evaluated for $z^2 = -r_k$, and N_0 is the total number of atoms.

5. High- and low-temperature expansions

Here we report high- and low-temperature expansions for the mean-square velocity of the isotope defect, and the defect energy per particle. Our results are derived from (19) and (21), respectively, in which the temperature T appears in $r_k = (2\pi kT)^2$, apart from a multiplicative factor. In the limit $\gamma \to 0$, when there is no modulation of the springs, our results agree with corresponding expressions reported by Maradudin *et al* (1971).

For high-temperature expansions we need $P(s;z)$ evaluated for $z \to \infty$ with $z^2 = -r_k$. To this end, we expand (6) in $(1/z^2)$, using (3) and (4) together with the eigenvalue equation. We find

$$mz^2P(s;z) = 1 + (\alpha_s + \alpha_{s+1})/mz^2 + \cdots \tag{22}$$

which substituted in (19) and (21) leads to

$$m'\langle v_s^2\rangle = T\{1 + (\alpha_s + \alpha_{s+1})/[12mT^2(1-\lambda)] + \cdots\} \tag{23}$$

and

$$\varepsilon(s) = \lambda(\alpha_s + \alpha_{s+1})/[12mTN_0(1-\lambda)] + \cdots \tag{24}$$

with α_n defined by (2). In these expressions we see the expected high-temperature limiting behaviour, in which $\langle v_s^2\rangle \to (T/m')$ and the defect energy vanishes. Impurity induced effects are seen to be most significant for a very light mass defect, namely $\lambda \to 1$. The defect energy has the sign of λ, so the internal energy is increased by a light defect and decreased by a heavy defect in accord with findings for site-independent springs.

In order to get low-temperature expansions from (19) and (21) we employ the Poisson summation formula,

$$\frac{h(0)}{2} + \sum_{k=1}^{\infty} h(k) = \sum_{m=-\infty}^{\infty} \int_0^{\infty} \mathrm{d}k\ h(k)\exp(2\pi imk) \tag{25}$$

in which it is assumed that $h(k) \to 0$ for $k \to \infty$. Inserting (25) in (19) and (21), integration by parts yields the zero-point contributions and a power series in T^2. Results to order T^2 are

$$\varepsilon(s) = \varepsilon_0(s) - \frac{T^2\pi F'(0)}{3N_0} + \mathrm{O}(T^4) \tag{26}$$

and

$$m(1-\lambda)\langle v_s^2\rangle = S_0 - \tfrac{1}{6}\pi^2 H'(0)T^2 + \mathrm{O}(T^4) \tag{27}$$

where the functions F and H are given by

$$F(u) = u^2\frac{\mathrm{d}}{\mathrm{d}u^2}\ln[1 - m\lambda u^2 P(s;\omega^2 = -u^2)]$$

and

$$H(u) = (2/m)[1 + m(1-\lambda)u^2 G(s;\omega^2 = -u^2)].$$

The zero-point values in (26) and (27) are

$$\varepsilon_0(s) = \frac{1}{\pi N_0}\int_0^\infty \mathrm{d}u\ F(u)$$

and

$$S_0 = \frac{1}{2}\int_0^\infty \mathrm{d}u\ H(u).$$

In order to evaluate the coefficients in these expansions it is convenient to use the Laurent expansion of (15)

$$mP(s;\omega^2 = -u^2) = A/u + Bu + Cu^3 + \cdots.$$

Differentiation then yields $F'(0) = -(\lambda A/2)$ and $H'(0) = 2m(1-\lambda)A/\pi$. We will require results for p_n and q_n evaluated at zero frequency:

$$p_n(0) = S_{n-1}(\alpha_{n-1}, \alpha_{n-2}, \ldots, \alpha_0)$$

and

$$q_n(0) = -\alpha_0^2 S_{n-2}(\alpha_{n-1}, \alpha_{n-2}, \ldots, \alpha_1)$$

where the function S_n takes $n+1$ arguments, forms all possible products of n distinct arguments and adds all these products together. These can be proved from (12) and yield the simple result

$$p_{N+1}(0) + q_N(0) = 2\alpha_{N-1}\alpha_{N-2}\ldots\alpha_0.$$

In order to evaluate A we also need the corresponding result for frequency derivatives in the form

$$p'_{N+1}(0) + q'_N(0) = -NS_{N-1}(\alpha_{N-1}, \alpha_{N-2}, \ldots, \alpha_0)$$

which can be proved using the Christoffel–Darboux formula.

These results then give

$$A = -\left[\frac{S_{N-1}(\alpha_{N-1}, \ldots, \alpha_0)}{4N\alpha_{N-1}\ldots\alpha_0}\right]^{1/2}$$

and substituting this in (26) and (27) we get the expansions

$$\varepsilon(s) = \varepsilon_0(s) - \frac{\pi\lambda}{6N_0}\left[\frac{S_{N-1}(\alpha_{N-1}, \ldots, \alpha_0)}{4N\alpha_{N-1}\ldots\alpha_0}\right]^{1/2} T^2 + \mathrm{O}(T^4) \tag{28}$$

and

$$m(1-\lambda)\langle v_s^2\rangle = S_0 + \frac{\pi(1-\lambda)}{3}\left[\frac{S_{N-1}(\alpha_{N-1}, \ldots, \alpha_0)}{4N\alpha_{N-1}\ldots\alpha_0}\right]^{1/2} T^2 + \mathrm{O}(T^4). \tag{29}$$

Note that the T^2 term is independent of the site s but the zero-point and T^4 terms are not. The zero-point integrals are dealt with in section 7 where results of extensive studies are presented.

6. Density of states

An analytic expression for the density of states in the pure system is given in (17). In general this is fragmented into N bands. The density of states in the system with a single defect at site s is given by modifying equation (16)

$$Z(\omega) = -\frac{2\omega}{\pi N_0} \sum_n m(1 - \lambda\delta_{n,s}) \operatorname{Im} G(n;\omega) \tag{30}$$

where $G(n;\omega)$ is the Green function provided in section 4. This formula yields

$$Z(\omega) = Z_p(\omega) - \left(\frac{2\omega}{\pi N_0}\right) \operatorname{Im} \frac{d}{d\omega^2} \ln[1 - m\lambda\omega^2 P(s;\omega)] \tag{31}$$

where $Z_p(\omega)$ denotes the density of states in the pure system (17)

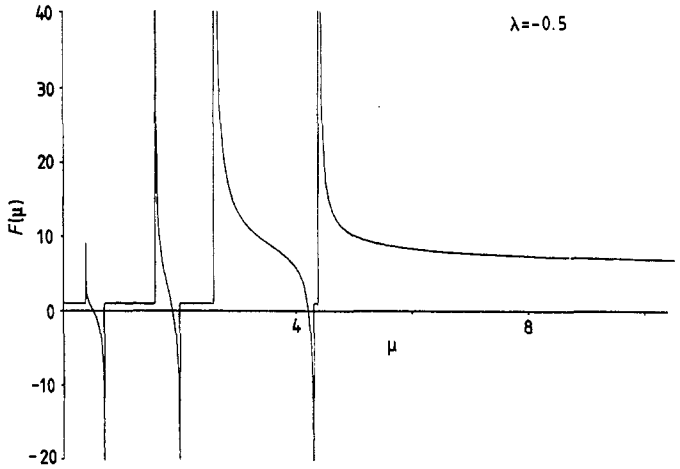

Figure 1. The function $f(\mu = \omega^2)$ defined in (33) for a defect at site $s = 0$. We take $\alpha = m = 1$, $N = 4$, $M = 1$, $\gamma + 0.5$, $\Delta = 0.0$ and $\lambda = -5.0$. The zeros of this function are the three localised modes for the system with a heavy mass defect and $N = 4$. Note that the unperturbed Green function has singularities at the band edges.

We now examine the changes in the density of states resulting from the defect given by the second contribution to $Z(\omega)$ in equation (31). Firstly we look at ω within the unstable bands of the pure system, i.e. frequencies such that $Z_p(\omega) = 0$. In this case we obtain

$$Z(\omega) = \frac{1}{N_0} \sum_i \delta(\omega - \omega_i) \tag{32}$$

where $\{\omega_i\}$ are the roots of

$$f(\omega^2) = \operatorname{Re}(1 - m\lambda\omega^2 P(s;\omega)) = 0. \tag{33}$$

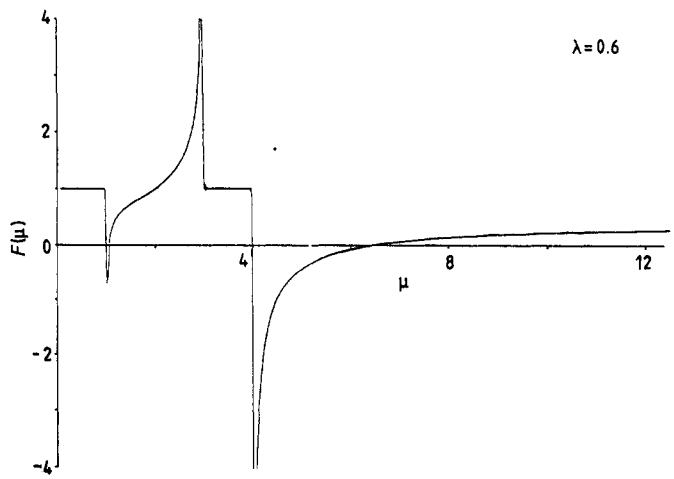

Figure 2. The function $f(\mu = \omega^2)$ given by (33) for a defect at site $s = 0$. We take $\alpha = m = 1$, $N = 2$, $M = 1$, $\gamma = 0.5$, $\Delta = 0.0$ and $\lambda = 0.6$. The zeros are the two localised modes for the system with a light mass defect and $N = 2$.

The $\{\omega_i\}$ are the frequencies of the so-called localised defect modes. Although the contribution (32) does not explicitly vanish in the limit $\lambda \to 0$ in fact it is trivial to show using (15) that $\{\omega_i\}$ move continuously to the edges of the stable bands as $\lambda \to 0$. In this way we can think of the localised defect modes as peeling off the edges of the stable bands. The roots of (33) have many interesting properties which can be extracted by studying the form of the Green function (15) and using properties of the polynomials $\{p_n\}$ and $\{q_n\}$ proved by Kato (1983). In particular, for $-\infty < \lambda < 0$ (heavy defect) there are $(N-1)$ localised modes, one just below each stable band. For a light defect, $0 < \lambda < 1$, there are N localised modes one just above each stable band. The function $f(\omega^2)$ is plotted in figure 1 for $\lambda < 0$ and $N = 4$ and in figure 2 for $\lambda > 0$ and $N = 2$; extensive numerical work is reported in the following section. The stable bands are identified by $f(\omega^2) = 1$, since the real part of the Green function vanishes in a band. Furthermore, the Green function is singular at band edges as is evident from the result (15) and the illustrations provided in figures 1 and 2. We can readily find the frequency of the highest localised mode, ω_o, for a light defect with $\lambda \to 1$. Taking just two term in the expansion (22) leads to

$$m\omega_0^2 = \frac{\alpha_s + \alpha_{s+1}}{(1/\lambda) - 1}. \tag{34}$$

Clearly as $\lambda \to 1$ the mode moves further from the band edge. The dependence on the parameters N, γ, and Δ is in the numerator of (34). There is no localised mode above the bands for a heavy defect.

Since the total number of modes is unchanged by the introduction of a substitutional defect, the normalisation of the density of states is preserved. In consequence, the intensity associated with the localised modes (32) is compensated by a decrease in intensity within the stable bands. The normalisation and width of the density of states is perhaps most easily tackled by exploiting the spectral representation of the

Green function. Starting from (6) it can be shown that

$$G(n;\omega) = -\frac{1}{\pi}\int_0^\infty \mathrm{d}u\ \frac{2u\,\mathrm{Im}\,G(n;u)}{\omega^2 - u^2}. \tag{35}$$

As the spectrum is bounded above we can safely expand the expression for large values of ω^2

$$G(n;\omega) = -\frac{1}{\pi\omega^2}\int_0^\infty \mathrm{d}u\ 2u\,\mathrm{Im}\,G(n;u) - \frac{1}{\pi\omega^4}\int_0^\infty \mathrm{d}u\ 2u^3\,\mathrm{Im}\,G(n;\omega) + \cdots. \tag{36}$$

The first term in (36) when summed over sites, as in (30) is proportional to the normalisation of the density of states, while the second term is the mean square width.

Using the explicit expansion given in (22) we can confirm that $Z(\omega)$ in the pure system is normalised to unity in $0 < \omega < \infty$. Expanding the defect contribution in (31)

$$\frac{\mathrm{d}}{\mathrm{d}\omega^2}\ln[1 - m\lambda\omega^2 P(s;\omega)] = (\lambda/m')(\alpha_s + \alpha_{s+1})\frac{1}{\omega^4} + \cdots \tag{37}$$

we see that there is no term in $1/\omega^2$. Hence, the integrated intensity from the mass defect is zero which is required to preserve the normalisation of the density of states. The contribution of the defect term to the mean-square width of the density of states is

$$(\lambda/m')(\alpha_s + \alpha_{s+1}) = [(m/m') - 1]\frac{(\alpha_s + \alpha_{s+1})}{m}.$$

This takes the sign of λ reflecting the fact that a heavy defect decreases all the normal-mode frequencies and a light defect increases them. The shift is large for $(m'/m) \to 0$ due to the emergence of a high-frequency localised mode (34) in this limit.

7. Numerical work

An explicit expression for the density of states for $N = 3$ has been reported by Lovesey (1989). For larger values of N the algebraic expressions become increasingly cumbersome. In view of this we turn to a wholly numerical implementation of our formulae in which the polynomials are obtained by straight forward recursion using (12) and appropriate initial values. We take as our example the case $N = 5$ and provide comparison with the results for $N = 3$.

Figure 3 shows the mean-square velocity of the defect atom as a function of reduced temperature. We take $\alpha = m = 1$, $\gamma = 0.5$, and $\Delta = 2\pi/5$. For these values of the parameters the five-periodic system has only three distinct sites. We show results for a defect at any one of these sites and for three values of the defect parameter λ. The most noticeable effect is seen by comparison of figures 3(b) and 3(c) with figure 3(a). Figure 3(a) corresponds to the pure system. We see that the distinction between the three sites increases for a light mass defect 3(c) and decreases for a heavy mass defect 3(b). Light mass defects therefore enhance the effect of the modulation. Further, we see that the mean-square velocity approaches classical values at high temperatures consistent with the expansions reported in section 5. The low-temperature limits

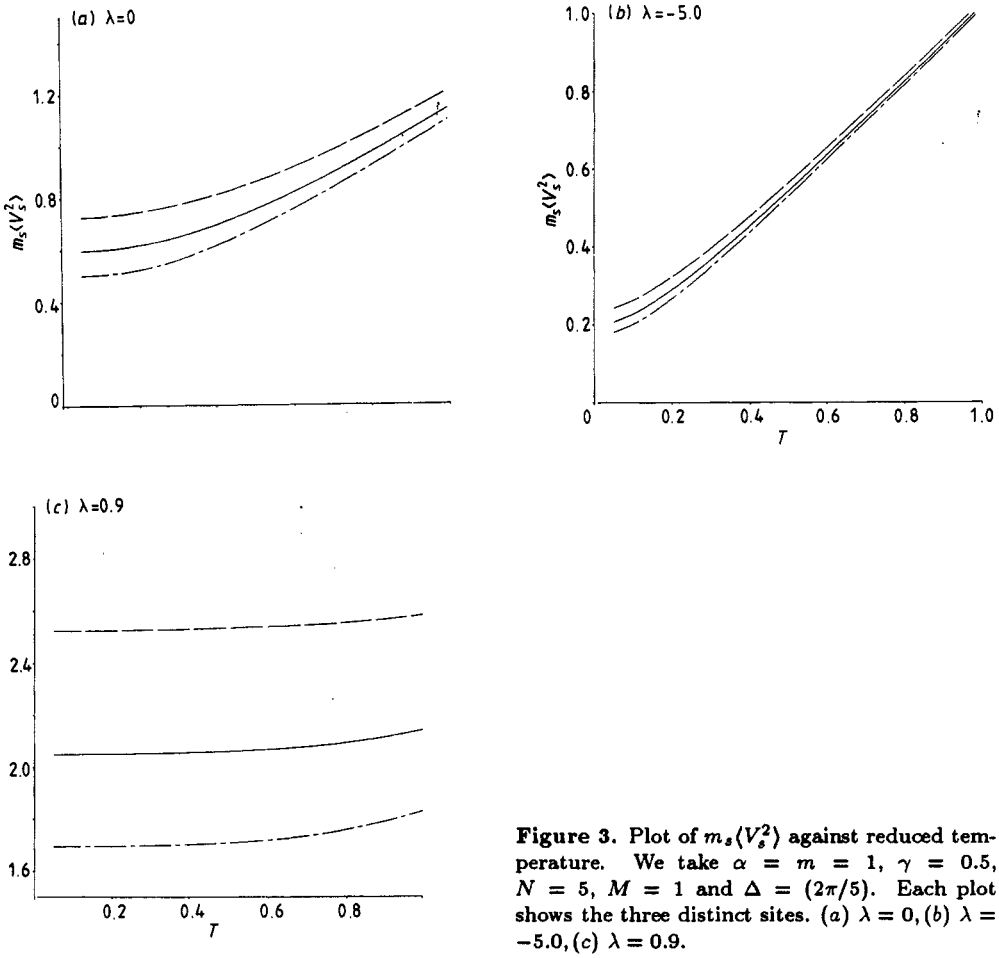

Figure 3. Plot of $m_s\langle V_s^2\rangle$ against reduced temperature. We take $\alpha = m = 1$, $\gamma = 0.5$, $N = 5$, $M = 1$ and $\Delta = (2\pi/5)$. Each plot shows the three distinct sites. (*a*) $\lambda = 0$, (*b*) $\lambda = -5.0$, (*c*) $\lambda = 0.9$.

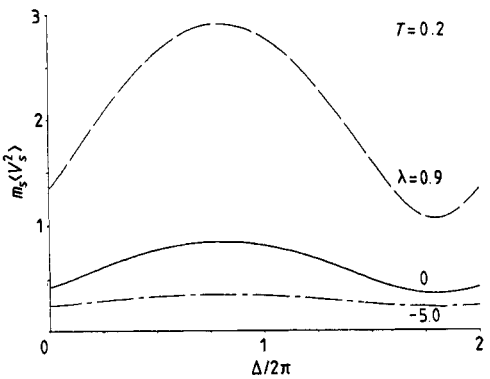

Figure 4. The quantity $m_s\langle v_s^2\rangle$ plotted against Δ/π is displayed for $\lambda = 0.0$, 0.9 and -5.0. We take $\alpha = m = 1$, $N = 5$, $M = 1$, $\gamma = 0.95$ and a temperature $T = 0.2$.

are consistent with the zero-point integral defined in section 5. In this context note

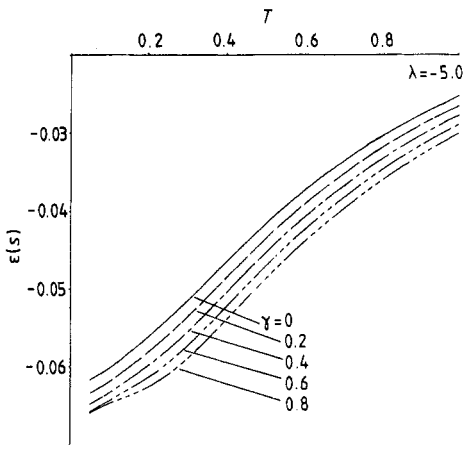

Figure 5. The defect energy, $\varepsilon(s)$, as a function of temperature for a heavy mass defect, $\lambda = -5.0$. Here the defect is at site $s = 0$ and we have $\alpha = m = 1$, $N = 5$, $M = 1$, $\gamma = 0.0 - 0.8$ and $\Delta = 2\pi/5$.

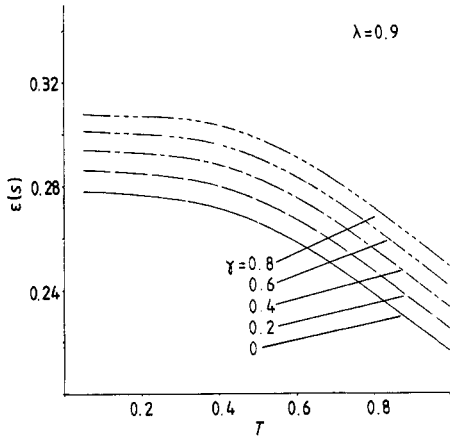

Figure 6. As figure 5, but for a light mass defect, $\lambda = 0.9$.

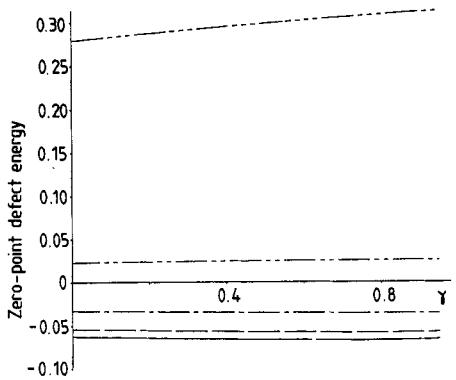

Figure 7. Zero-point defect energy against γ for $\alpha = m = 1$, $N = 5$, $M = 1$, $\Delta = 2\pi/5$. The defect is at site $s = 0$. Various values of λ are considered.

that for $\lambda = 0.9$ (figure 3(*c*)) the low-temperature behaviour is constant to a good approximation in contrast to the results reported by Lovesey (1989); the difference in behaviour has been traced to an inadequate numerical scheme in the latter work.

In figure 4 we examine the effect of the phase of the modulation Δ on the mean-square velocity. The broad features are the same for $N = 3$ and $N = 5$ in the sense that in each case there is one maximum and one minimum in the range $0 < \Delta < 2\pi$. Again we see that light defects enhance the effect of the modulation while heavy defects reduce it.

We now turn our attention to the defect energy, $\varepsilon(s)$. It is shown as a function of temperature in figures 5 and 6 for various values of the modulation γ. For a heavy defect $\varepsilon(s)$ is negative, while for a light defect it is positive. If we take a light defect (figure 8) we see that defect energy is an increasing function of the modulation γ. For the heavy defect the defect energy is a decreasing function of γ except at very low

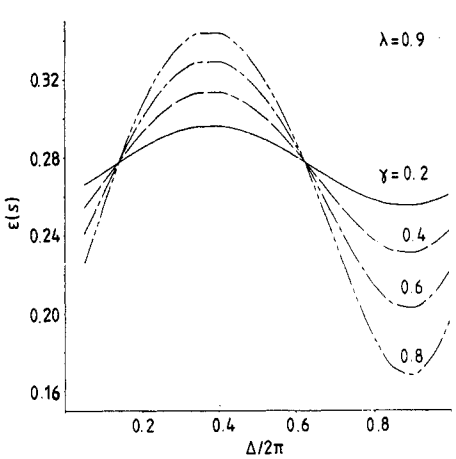

Figure 8. The defect energy as a function of $\Delta/2\pi$ at a temperature $T = 0.2$ for a light defect, $\lambda = 0.9$. Again $\alpha = m = 1$, $N = 5$, $M = 1$ and we show $\gamma = 0.0 - 0.8$.

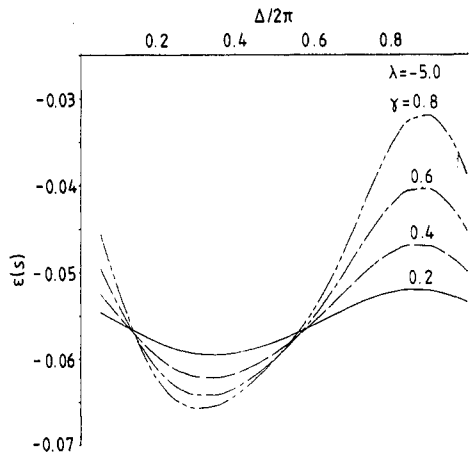

Figure 9. As figure 8, but for a heavy defect, $\lambda = -5.0$. Note the significant difference in the vertical scales compared with figure 8.

temperatures where it is no longer a monatonic function but shows a minimum for an intermediate value of γ.

These results should be compared with figure 7 which shows the zero-point defect energy as a function of γ. Clearly it is monatonic increasing for $\lambda > 0$ but shows a weak minimum for $\lambda < 0$.

Finally in figures 8 and 9 we show defect energy as a function of modulation phase Δ at a temperature $T = 0.2$ and for various values of γ. The salient features do not change from $N = 3$ to $N = 5$, in as much as that there is one distinct maximum and one distinct minimum. Clearly a defect will lock to the modulation phase at the value corresponding to minimum defect energy. While the size of the lock-in effect is exaggerated for small periodicities it is expected to survive in the incommensurate limit.

8. Conclusions

An algebraic method, imported from our previous studies of modulated magnets and electrons in a magnetic field, provides an elegant means of obtaining thermodynamic properties of the modulated spring chain. Attention here is limited to a cosine modulation, but the same method is successful for more complicated modulation functions, as demonstrated by Lovesey and Westhead (1990). A major part of the work reported has addressed properties of a mass defect in the modulated chain. Without exception we find that effects due to the spring modulation are enhanced by exploiting a probe with mass less than the host atoms. It is shown that a mass defect generates a localised mode in every gap in the fragmented density of states, and for a light mass there is an additional one above the highest frequency band. Thermodynamic properties have been obtained without recourse to standard integrals of the density of states for these would clearly be technically difficult to accurately perform. High- and

low-temperature expansions reveal the sensitivity of thermodynamic quantities to the modulation. As might be expected, this is largest at low temperatures.

Acknowledgments

One of us (DRW) is grateful for the award of an SERC studentship. We have benefitted from discussions with Drs Lennart Häggström and Paul Vulliet.

Appendix

Equation (15) gives an expression for the Green function in terms of the sets of polynomials $\{p_n\}$ and $\{q_n\}$. In this appendix we present a derivation of this equation which follows Lovesey 1988a, b fairly closely but also provides a prescription for choosing the sign on the right hand side of (15).

Beginning with the equation of motion (7) it is a matter of trivial manipulation to produce an exact expression for the Green function in terms of two infinite continued fractions

$$mP(n;z) = \frac{1}{\Omega_n - \alpha_n^2 G_n - H_{n+1}} \tag{A1}$$

where $\Omega_n = z^2 - \alpha_n - \alpha_{n+1}$, and

$$H_n = \cfrac{\alpha_n^2}{\Omega_n - \cfrac{\alpha_{n+1}^2}{\Omega_{n+1} - \cfrac{\alpha_{n+2}^2}{\Omega_{n+2} - \cdots}}} \tag{A2}$$

$$G_n = \cfrac{1}{\Omega_n - \cfrac{\alpha_{n-1}^2}{\Omega_{n-2} - \cfrac{\alpha_{n-2}^2}{\Omega_{n-3} - \cdots}}} \tag{A3}$$

Considerable simplification is produced by taking the coefficients in these continued fractions to be periodic, ie $\alpha_{n+N} = \alpha_n$. In this case $H_0 \equiv H$ and $G_0 \equiv G$ can be shown to correspond to fixed points of bilinear transformations and we can produce closed algebraic formulae for the continued fractions.

In order to deal with H it is natural to introduce a set of transformations $\{J_n\}$ defined by

$$J_n(x) = \alpha_0^2/\{\Omega_0 - \alpha_1^2/[\Omega_1 - \ldots - \alpha_{n-1}^2/(\Omega_{n-1} - x)]\}. \tag{A4}$$

These can be expressed in terms of the polynomials $\{p_n\}$ and $\{q_n\}$ defined in section 3,

$$J_n(x) = \frac{q_{n+1} + xq_n}{p_{n+1} + xp_n}. \tag{A5}$$

This can be proved by induction, it is clearly a bilinear transformation.

It is clear that if H converges then it is a fixed point of the N-fold transformation; $J_N(H) = H$. This condition is stated more precisely in the following theorem due to Wall (see Wall (1973), theorem 8.1).

Let x_1 and x_2 be the two fixed points of J_N, and let F_n be the *nth* approximant of H defined by $F_n = J_n(0) = q_{n+1}/p_{n+1}$. Then H converges if and only if x_1 and x_2 are finite complex numbers satisfying either

$$x_1 = x_2$$

or

$$|F_{N-1} - x_2| > |F_{N-1} - x_1| \qquad F_p \neq x_2$$

for $p = 0, 1, \ldots, N-1$. If the continued fraction converges it's value is x_1.

The two fixed points of J_N are given by (A5), they satisfy the quadratic equation

$$x^2 p_N + x(p_{N+1} - q_N) - q_{N+1} = 0 \tag{A6}$$

i.e.

$$x_1, x_2 = (q_N - p_{N+1} \pm \sqrt{-D_N})/2p_N \tag{A7}$$

where we have used (13) and (14). The above theorem requires x_1 (the value of H) to be the root that minimises

$$|F_{N-1} - x_1, x_2| = |p_{N+1} + q_N \mp \sqrt{-D_N}|/2|p_N|. \tag{A8}$$

Outside the stable bands where $D_N < 0$ this can be implemented straightforwardly. If $p_{N+1} + q_N > 0$ then

$$x_1 = H = (q_N - p_{N+1} + \sqrt{-D_N})/2p_N \tag{A9}$$

and if $p_{N+1} + q_N < 0$ then

$$x_1 = H = (q_N - p_{N+1} - \sqrt{-D_N})/2p_N. \tag{A10}$$

It is easy to show that the polynomial $p_{N+1} + q_N$ has no roots in the regions $D_N < 0$.

Within the stable bands the situation is complicated by the fact that the continued fractions do not converge for D_N real, $D_N > 0$. In order to obtain convergent continued fractions we must assign D_N a small imaginary part, corresponding to $z = \omega + i\eta$ where $\eta \to 0^+$. We have

$$-D_N(z) = -\left(D_N(\omega) + i\eta \frac{dD_N}{d\omega}\right) \tag{A11}$$

and we use the notation $b = -\eta\, dD_N/d\omega$. Using this prescription, minimisation of the quantity given in equation (A8) leads us to minimise

$$\left| p_{N+1} + q_N \mp \frac{b}{2\sqrt{D_N}} \right|. \tag{A12}$$

If x_1 is the root that accomplishes this, then for $p_{N+1} + q_N > 0$ the sign that we take in (A7) to correspond to x_1 is that of $+b$, and for $p_{N+1} + q_N < 0$ we take the sign of $-b$. In this way we have an algebraic expression for H on the full real axis of the D_N plane.

The above analysis can be repeated for the other continued fraction G. This yields the result that $1/G$ is given by the same quadratic equation as H, the equation (A6), but corresponds to the other root x_2. The sum and product of these roots are then given by

$$\frac{H}{G} = -\frac{q_{N+1}}{p_N} \tag{A13}$$

and

$$H + \frac{1}{G} = -\frac{p_{N+1} - q_N}{p_N}. \tag{A14}$$

The difference of the roots is given by

$$H - \frac{1}{G} = \frac{\pm\sqrt{-D_N}}{p_N} \tag{A15}$$

and the sign of this is to be chosen according to the above prescription for deciding which root is x_1.

Noting that equation (A4) implies that $J_n(H_n) = H$, and using this in (A5) we obtain

$$H = \frac{q_{n+1} + H_n q_n}{p_{n+1} + H_n p_n}. \tag{A16}$$

We can obtain a similar expression for G_n in terms of G, and substitute these in (A1) to yield the following expression for the Green function in terms of the quantities above

$$mP(n;z) = \frac{-p_{n+1}^2(H/G) + p_{n+1}q_{n+1}(H + 1/G) - q_{n+1}^2}{\alpha_n^2\alpha_{n-1}^2 \ldots \alpha_0^2(H - 1/G)}. \tag{A17}$$

Substituting for these quantities we obtain equation (15)

$$mP(n;z) = \frac{\pm[q_{N+1}p_{n+1}^2 + p_{n+1}q_{n+1}(q_N - p_{N+1}) - p_N q_{n+1}^2]}{\alpha_n^2\alpha_{n-1}^2 \ldots \alpha_0^2\sqrt{D_N}}.$$

Outside the stable bands we use equations (A9) and (A10) to chose the sign in (15) to be positive if $p_{N+1} + q_N > 0$, and negative if $p_{N+1} + q_N < 0$.

Within the stable bands we are concerned to prove that our expression for the density of states, given in (16), is strictly positive. For $D_N > 0$, substituting (15) in (16), and using the Christoffel—Darboux formula (see Lovesey 1988a,b), we obtain

$$Z(\omega) = \frac{\pm 2\omega(p'_{N+1} + q'_N)}{\pi N\sqrt{D_N}} \tag{A18}$$

where the prime denotes differentiation with respect ω^2. This can be rewritten

$$Z(\omega) = \frac{\mp\omega D'_N}{\pi N(p_{N+1}+q_N)\sqrt{D_N}}. \tag{A19}$$

In this way the sign of $Z(\omega)$ is related to the sign of $p_{N+1}+q_N$, the sign of $\omega D'_N$, and our choice of sign in (15). Noting that $b = -\eta\ \mathrm{d}D_N/\mathrm{d}\omega = -2\eta\omega D'_N$ we can try out all possibilities for the signs of the various quantities and it emerges that the analysis will always yield a density of states that is strictly positive within the stable bands, as in equation (17).

References

Currat R and Janssen T 1988 *Solid State Physics* vol 41 (New York: Academic) p 201
de Lange C and Janssen T 1981 *J. Phys. C: Solid State Phys.* **14** 5269
Kato Y 1988 *Proc. RIMS Symposium (Kyoto)* (Singapore: World Scientific)
Lovesey S W 1986 *Condensed Matter Physics: Dynamic Correlations (Frontiers in Physics 61)* (Menlo Park, CA: Benjamin/Cummings)
—— 1987 *Theory of Neutron Scattering from Condensed Matter* vol 1 (Oxford: Oxford University Press)
—— 1988a *J. Phys. C: Solid State Phys.* **21** 2805
—— 1988b *J. Phys. C: Solid State Phys.* **21** 4967
—— 1989 *J. Phys.: Condens. Matter* **1** 2731
Lovesey S W and Westhead D R 1990 *J. Phys.: Condens. Matter* **2** 7425–34
Maradudin A A, Montroll E W, Weiss G H and Ipatova I P 1971 *Solid State Physics* Suppl. 3 2nd edn (New York: Academic)
Rubin R J 1961 *J. Math. Phys.* **2** 373
Wall H S 1973 *Continued Fractions* (Bronx, NY: Chelsea)